ANALYTIC FORMULA FOR THE DIFFERENCE OF THE CIRCUMRADIUS AND ORTHORADIUS OF A WEIGHTED TRIANGLE

Michelle H. Hummel

Sandia National Laboratories, Albuquerque, NM, mhhumme@sandia.gov

ABSTRACT

Understanding and quantifying the effects of vertex insertion, perturbation, and weight allocation is useful for mesh generation and optimization. For weighted primal-dual meshes, the sensitivity of the orthoradius to mesh variations is especially important. To this end, this paper presents an analytic formula for the difference between the circumradius and orthoradius of a weighted triangle in terms of edge lengths and point weights under certain weight and edge assumptions. Current literature [1] offers a loose upper bound on the this difference, but as far as we know this is the first formula presented in terms of edge lengths and point weights. A formula in these terms is beneficial as these are fundamental quantities which enable a more immediate determination of how the perturbation of a point location or weight affects this difference. We apply this result to the VoroCrust algorithm to obtain the same quality guarantees under looser sampling conditions.

Keywords: mesh generation, computational geometry, weighted Delaunay triangulation, Voronoi tessellation

1. INTRODUCTION

A quality mesh is important in a variety of applications such as computer graphics, scientific and engineering simulations, and geometric modeling. Mesh generation algorithms based on Delaunay triangulations are advantageous because of their well-developed theory and algorithms [2, 3, 4, 5, 6, 7, 8], fast vertex insertion [5], and optimality properties with respect to interpolation and maximization of minimum angles [9]. In addition, Delaunay triangulations have an orthogonal dual mesh, the Voronoi tesselation. Many geometry processing applications rely on the dual structure of the Delaunay triangulation [10].

A Delaunay triangulation has the property that the interior of the circumball of each triangle is empty of other vertices in the triangulation. A Voronoi tessellation is a partition of the space into Voronoi cells. A Voronoi cell corresponding to a specific vertex (cell generator) is defined as the region for which the distance to the cell generator is less than or equal to the distance to all other vertices in the triangulation. By adding weights to the vertices, the Delaunay/Voronoi primal/dual mesh is generalized to the weighted-Delaunay/weighted-Voronoi primal/dual mesh [5]. A weighted-Voronoi diagram is also known as a power diagram. In the context of a weighted-Voronoi tessellation, a larger weight corresponds to a relatively larger weighted-Voronoi cell. Vertex weights also provide control over other properties of the orthogonal dual mesh such as the location of the dual vertices, how well-centered a mesh is, the shape of dual cells, and are important for applications such as the generation of well-centered meshes, sphere packing, and self-supporting surfaces [10, 11].

Delaunay refinement, where vertices are added to a Delaunay triangulation or a constrained Delaunay triangulation, vertex perturbation [2], and smart weight assignment to existing vertices are common Delaunay-based methods to build a suitable mesh (see [1] for a discussion on this subject). In particular, introduction of appropriate point weights are important for primal-dual meshes, especially when a well-centered mesh is desired [10]. Furthermore, polyhedral meshing methods based on the Voronoi tesselation, for example the VoroCrust [12, 13], and power crust algorithms [14, 15], utilize a sample of weighted points in the mesh building process. Thus it is desirable to understand how a Delaunay mesh changes with respect to vertex insertion and perturbation, and weight perturbation. In particular, the difference between circumradius and weighted circumradius (orthoradius) is useful for mesh optimization. For example, Engwirda [11] uses a quality metric that directly measures the distance between circumcenter and orthocenter, a quantity that can be bounded using our formula, for a mimetic formulation of ocean climate simulations.

Cheng et. al [1] show that the circumradius of a triangle is bounded by a constant times its orthoradius. In particular, if $\triangle s_1 s_2 s_3$ has circumradius R and orthoradius $\hat{R}$, where s_i has weight $w_i \in [0, \alpha^2 N(s_i)^2]$ for $\alpha \in [0, 1/2)$ and $N(s_i)$ is the distance from s_i to its nearest vertex, then $R \leq c_{\rm rad}\hat{R}$, where $c_{\rm rad} = 1/\sqrt{1-4\alpha^2}$. This result gives a constant upper bound on radius-edge ratio, one measure of mesh quality. However, the bound is not tight and the authors conjecture that the bound can be improved to $c_{\rm rad} = 1/\sqrt{1-3\alpha^2}$. Additionally, a formula in terms of edge lengths and point weights is beneficial as these are more fundamental quantities than the radius-edge ratio. Furthermore, the radius depends on the location of three vertices whereas an edge length depends on only two. Thus, it is more immediately clear how the perturbation of a point location or weight affects the difference between the circumradius and orthoradius.

In this paper, we give an analytic formula for the difference of the circumradius and orthoradius of a weighted triangle under slightly relaxed conditions on point weights and edge lengths. Specifically, this assumption is that the magnitude of the differences between point weights is less than or equal to the edge length squared. Such limits on spacing and weights are common, as in standard sparse sampling algorithms [16]. We then apply our result to the VoroCrust method in Abdelkader et al. [12].

2. STATEMENT OF PROBLEM

In this paper we find a formula for $R - \hat{R}$ where R is the circumradius of a weighted triangle and $\hat{R}$ is the orthoradius, under minor assumptions on point weights and edge lengths. We write $t_s = (s_i, s_j, s_k)$ where each s_i is a weighted point $s_i = (s_i', s_i'')$. The point s_i may be interpreted as a ball with center s_i' and weight or squared radius of s_i''. Note that s_i'' may be negative.

We assume that the differences in point weights is small compared to edge lengths. In particular,

$$\frac{|s_i'' - s_j''|}{|s_i' - s_j'|^2} \leq 1 \quad \forall \quad s_i, s_j \in t. \tag{1}$$

Such limits on spacing and weights are common, as in standard sparse sampling algorithms [16].

The characteristic point or orthoball, $\hat{Z} = (\hat{z}, \hat{R}^2)$, of t_s is defined as

$$\Pi(s_i, \hat{Z}) := (s_i' - \hat{z})^2 - \hat{R}^2 - s_i'' = 0 \qquad \forall s_i \in t_s. \tag{2}$$

The circumball, $Z = (z, R^2)$, of t is defined as

$$(s_i' - z)^2 - R^2 = 0 \qquad \forall s_i \in t. \tag{3}$$

Define $t(\alpha) = (s_i(\alpha), s_j(\alpha), s_k(\alpha))$ where $s_i(\alpha) = (s_i', s_i'' - \alpha)$ for all $s_i(\alpha) \in t_s(\alpha)$. The orthoball is

$$\hat{Z}(\alpha) = (\hat{z}, \hat{R}^2 + \alpha). \tag{4}$$

That is the orthoball, $\hat{Z}(\alpha) = (\hat{z}(\alpha), \hat{R}^2(\alpha))$, of $t(\alpha)$ satisfies

$$\begin{aligned} \hat{z}(\alpha) &= \hat{z} \\ \hat{R}^2(\alpha) &= \hat{R}^2 + \alpha. \end{aligned} \tag{5}$$

3. DERIVATION OF DIFFERENCE

Without loss of generality, assume s_i is the vertex with the smallest weight α. That is, $\alpha = s_i'' = \min(s_i'', s_j'', s_k'')$. Due to the relationship shown in (5), we change the weights by α so one vertex has weight zero and the other two vertex weights are non-negative. In particular, consider the triangle $t_s(\alpha) = t = (p_i, p_j, p_k)$ where

$$\begin{aligned} p_i = (s_i', s_i'' - \alpha) &= (A, 0) \\ p_j = (s_j', s_j'' - \alpha) &= (B, w_B) \\ p_k = (s_k', s_k'' - \alpha) &= (C, w_C). \end{aligned} \tag{6}$$

The triangle t has the same orthocenter as t_s and orthoradius $\hat{R}^2 = \hat{R}_s^2 + \alpha$ where $\hat{R}_s$ is the orthoradius of t_s.

We define the edge lengths

$$a = |BC| \tag{7}$$

$$b = |CA| \tag{8}$$

$$c = |AB| \tag{9}$$

and

$$\theta = \angle CAB \tag{10}$$

as shown in Figure 1.

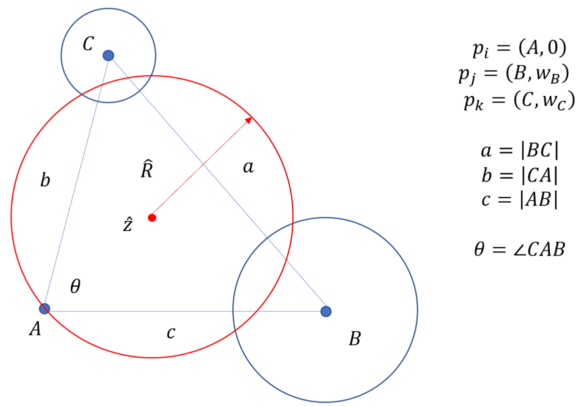

Figure 1: The weighted triangle $t = (p_i, p_j, p_k)$, with edge lengths a, b, c, and orthoball $\hat{Z} = (\hat{z}, \hat{R}^2)$.

Note that the assumption in (1) ensures that the boundary of the ball $\hat{Z}$ intersects the triangle edges. The point $\hat{Z}$ is the circumball of the set of unweighted points $\hat{t} = (\hat{A}, \hat{B}, \hat{C})$ where $\hat{A} = A$ as shown in Figure 2.

We also define

$$\begin{aligned} \hat{a} &= |\hat{B}\hat{C}| & (11)\\ \hat{b} &= |\hat{C}\hat{A}| & (12)\\ \hat{c} &= |\hat{A}\hat{B}|. & (13) \end{aligned}$$

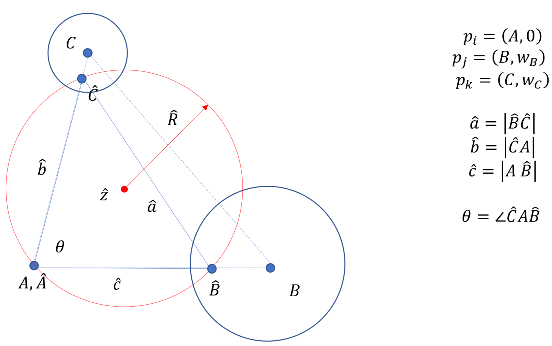

Figure 2: The orthoball $\hat{Z}$ of t is also the circumball of $\triangle\hat{A}\hat{B}\hat{C}$ with edge lengths $\hat{a}$, $\hat{b}$, and $\hat{c}$. Without loss of generality, the vertex A is associated with the minimum vertex weight for the triangle. Thus, as shown by (6) we have $A = \hat{A}$.

The areas of the triangles defined by t and $\hat{t}$ are respectively

$$M = bc\frac{\sin\theta}{2}, \quad \hat{M} = \hat{b}\hat{c}\frac{\sin\theta}{2}. \tag{14}$$

In addition,

$$R = \frac{abc}{4M}, \quad \hat{R} = \frac{\hat{a}\hat{b}\hat{c}}{4\hat{M}} \tag{15}$$

which gives

$$R - \hat{R} = \frac{a - \hat{a}}{2\sin\theta} \tag{16}$$

and

$$\frac{R - \hat{R}}{R} = \frac{a - \hat{a}}{a}. \tag{17}$$

In order to estimate $a - \hat{a}$, we find δ_b and δ_c where $b = \hat{b} + \delta_b$ and $c = \hat{c} + \delta_c$. The characteristic point x_e of the edge $\sigma_e = \overline{AB}$ satisfies

$$\begin{aligned} |x_e' - p_i'|^2 - x_e'' &= 0\\ |x_e' - p_j'|^2 - x_e'' - p_j'' &= 0 & (18) \end{aligned}$$

with x_e'' minimal. From [17] we have

$$x_e' = tA + (1-t)B \tag{19}$$

with

$$t = \frac{1}{2}(1 + \frac{w_B}{c^2}). \tag{20}$$

Combining (19) and (20) gives

$$x_e' = \frac{1}{2}(A+B) + \frac{w_B}{2c^2}(A-B). \tag{21}$$

We also have

$$x_e' = A + \frac{\sqrt{x_e''}}{c}(B-A) \tag{22}$$

which with (21) gives

$$c = 2\sqrt{x_e''} + \frac{w_B}{c}. \tag{23}$$

Additionally,

$$\hat{c} = 2\sqrt{x_e''} \tag{24}$$

which gives

$$\delta_c = c - \hat{c} = \frac{w_B}{c} \tag{25}$$

$$\delta_b = b - \hat{b} = \frac{w_C}{b}. \tag{26}$$

From the law of cosines

$$\hat{a}^2 = \hat{b}^2 + \hat{c}^2 - 2\hat{b}\hat{c}\cos\theta \tag{27}$$

and

$$\begin{aligned} a^2 &= b^2 + c^2 - 2bc\cos\theta\\ &= (\hat{b}+\delta_b)^2 + (\hat{c}+\delta_c)^2 - 2(\hat{b}+\delta_b)(\hat{c}+\delta_c)\cos\theta\\ &= (\hat{b}^2 + \hat{c}^2 - 2\hat{b}\hat{c}\cos\theta) + 2\hat{b}\delta_b + 2\hat{c}\delta_c + \delta_b^2 + \delta_c^2\\ &\quad -2(\hat{b}\delta_c + \hat{c}\delta_b + \delta_b\delta_c)\cos\theta\\ &= \hat{a}^2 + (2\hat{b}\delta_b + 2\hat{c}\delta_c + \delta_b^2 + \delta_c^2)\\ &\quad -2(\hat{b}\delta_c + \hat{c}\delta_b + \delta_b\delta_c)\cos\theta\\ &= \hat{a}^2 + 2(w_B + w_C) - (\frac{w_B}{c})^2 - (\frac{w_C}{b})^2\\ &\quad -2(\frac{bw_B}{c} + \frac{cw_C}{b} - \frac{w_B w_C}{bc})\cos\theta\\ &:= \hat{a}^2 + k. & (28) \end{aligned}$$

This gives

$$R - \hat{R}(\alpha) = \frac{a - \sqrt{a^2 - k}}{2\sin\theta} \leq \frac{\sqrt{k}}{2\sin\theta} \quad (29)$$

and

$$\frac{R - \hat{R}(\alpha)}{R} = \frac{a - \sqrt{a^2 - k}}{a} \leq \frac{\sqrt{k}}{a} \quad (30)$$

where

$$\begin{aligned} k &= 2(w_B + w_C) - (\frac{w_B}{c})^2 - (\frac{w_C}{b})^2 \\ &\quad -2(\frac{cw_C}{b} + \frac{bw_B}{c} - \frac{w_B w_C}{bc})\cos\theta. \end{aligned} \quad (31)$$

Theorem 1. *Given a weighted triangle $s = (s_i, s_j, s_k)$ and under the assumption of (1), the difference between the circumradius and orthoradius is given by*

$$R - \hat{R} = \frac{a - \sqrt{a^2 - k}}{2\sin\theta} + s_i'' \quad (32)$$

where $s_i'' = \min(s_i'', s_j'', s_k'')$, the constant k is given in (31), $w_B = s_j'' - s_i''$, and $w_C = s_k'' - s_i''$.

4. APPLICATIONS

This result may be applied to a variety of applications. In this paper, we apply our result to the VoroCrust algorithm discussed in "Sampling Conditions for Conforming Voronoi Meshing by the VoroCrust Algorithm" [12]. In Section 4.1, we use Theorem 1 to obtain the same quality guarantees with looser sampling criterion. The results may also be applied to [13] to improve termination criterion. Looser sampling and improved termination criteria result in a coarser mesh with fewer elements as well as a reduced algorithm run time.

Numerous publications rely on previously published bounds. For example, the 2012 text containing Cheng's bound [1], which we discussed in Section 1 has 400 citations. While all citations most likely do not involve the bound, it shows that there is high interest in this topic. A more general bound is potentially useful in a lot of contexts in addition to VoroCrust.

4.1 VoroCrust

We apply this result to the VoroCrust algorithm as given in Abdelkader et al. [12]. An ϵ-sampling, $\mathcal{P}$, which is σ-sparse is obtained on a surface $\mathcal{M}$ which is 1-Lipschitz with respect to local feature size L. Each point in $\mathcal{P}$ is associated with a radius which is given by $\delta = 2\epsilon$ times the local feature size. The set $\mathcal{P}$ along with their weights defines a weighted Delaunay triangulation which consists of "guide triangles". The set $\mathcal{S}$ contains sites which are the intersection points of three spheres corresponding to triangles in the weighted Delaunay triangulation. These sites are the generators for the Voronoi cells. A subset of these facets, $\hat{\mathcal{M}}$, approximate the surface $\mathcal{M}$. It is required that the orthocenter of a triangle lies within a certain distance of the surface $\mathcal{M}$. Given a guarantee that the circumcenter of the triangle lies within a given distance, one may guarantee that the orthocenter lies within a certain distance using the difference between circumradius and orthoradius.

The sampling conditions for $\mathcal{P}$ are as follows: for all $x \in \mathcal{M}$ there exists $p_i' \in \mathcal{P}$ such that $|x - p_i'| < \epsilon L(x)$ and $|p_i' - p_j'| \geq \sigma\epsilon \min(L(p_i'), L(p_j'))$. The parameter σ is set to 3/4.

Consider the guide triangle $t = (p_i, p_j, p_k)$. Let $L_i = L(p_i)$, the local feature size at p_i. Without loss of generality, assume that $L_i \leq L_j \leq L_k$. We subtract the minimum weight $\delta^2 L_i^2$ from all points in t to obtain the scenario given in the previous section.

From sparsity and as shown in [18] Property H3, we have $R \leq \frac{\epsilon}{1-\epsilon} L_i$ which gives an upper bound of $2\frac{\epsilon}{1-\epsilon} L_i$ on edge lengths. By Lipschitz, this gives

$$L_j \leq \frac{1+\epsilon}{1-\epsilon} L_i. \quad (33)$$

and similarly for L_k. Combining the upper bound on edge lengths, sparsity conditions, and Lipschitz we obtain

$$\sigma\epsilon L_i \leq \quad d(p_i, p_j) = c \leq \quad 2\frac{\epsilon}{1-\epsilon} L_i \quad (34)$$

$$\sigma\epsilon L_i \leq \quad d(p_i, p_k) = b \leq \quad 2\frac{\epsilon}{1-\epsilon} L_i \quad (35)$$

$$\sigma\epsilon L_i \leq \quad d(p_j, p_k) = a \leq \quad 2\frac{\epsilon(1+\epsilon)}{(1-\epsilon)^2} L_i. \quad (36)$$

The weight

$$\begin{aligned} w_B &= \delta^2(L_j^2 - L_i^2) && (37) \\ &\leq \frac{16\epsilon^3}{(1-\epsilon)^2} L_i^2 && (38) \end{aligned}$$

and similarly for w_c. This gives

$$0 \leq \quad w_B \quad \leq \frac{16\epsilon^3}{(1-\epsilon)^2} L_i^2 \quad (39)$$

$$0 \leq \quad w_C \quad \leq \frac{16\epsilon^3}{(1-\epsilon)^2} L_i^2. \quad (40)$$

Write

$$k = k_1 + k_2 \cos\theta \quad (41)$$

where

$$k_1 \quad := \quad 2(w_B + w_C) - (\frac{w_B}{c})^2 - (\frac{w_C}{b})^2 \quad (42)$$

$$k_2 \quad := \quad -2(\frac{cw_C}{b} + \frac{bw_B}{c} - \frac{w_B w_C}{bc}). \quad (43)$$

Then using bounds on edge lengths and weights,

$$k_1 \leq 2^6 \frac{\epsilon^3}{(1-\epsilon)^2} L_i^2 \tag{44}$$

and

$$\frac{-2^7 \epsilon^3 L_i^2}{\sigma(1-\epsilon)^3} \leq k_2 \leq \frac{2^9 \epsilon^4 L_i^2}{\sigma^2(1-\epsilon)^4}. \tag{45}$$

Then

$$\begin{aligned} k &\leq 2^6 \frac{\epsilon^3}{(1-\epsilon)^2} L_i^2 \\ &+ \begin{cases} UB(k_2)UB(\cos\theta) \text{ if } \theta \leq \pi/2 \\ LB(k_2)LB(\cos\theta) \text{ if } \theta > \pi/2 \end{cases} \end{aligned} \tag{46}$$

where UB and LB denote the upper bound and lower bound, respectively.

From the Central Angle Theorem we have

$$\sin(\theta) = \frac{a}{2R}. \tag{47}$$

This gives

$$\begin{aligned} \sin(\theta) &= \frac{a}{2R} \\ &\geq \frac{\sigma(1-\epsilon)}{2} \\ &:= k_{\text{sin}}. \end{aligned} \tag{48}$$

We may use the law of cosines to get a lower bound for $\cos\theta$,

$$\begin{aligned} \cos\theta &= \frac{b^2 + c^2 - a^2}{2bc} \\ &\geq 1/4\sigma^2(1-\epsilon)^2 - 1/2\frac{(1+\epsilon)^2}{(1-\epsilon)^2} \\ &:= k_{cos}. \end{aligned} \tag{49}$$

Note that $k_{cos} < 0$.

Then if $\theta \leq \pi/2$

$$\sin\theta \geq k_{sin} \tag{50}$$

$$\cos\theta \leq \sqrt{1 - k_{sin}^2} \tag{51}$$

and if $\theta > \pi/2$

$$\sin\theta \geq \sqrt{1 - k_{cos}^2} \tag{52}$$

$$\cos\theta \geq k_{cos}. \tag{53}$$

Plugging these bounds for $\cos\theta$ and $\sin\theta$ into (46) along with Theorem 1 gives the desired bound. The results using the inequality $a - \sqrt{a^2 - k} \leq \sqrt{k}$ are shown in Figure 3.

This result may be used to obtain the same quality guarantees obtained in [12] but for larger ϵ. In particular, Lemma 9 bounds R by

$$R \leq \rho_f \hat{R} \tag{54}$$

with $\rho_f < 1.38$. The orthoradius is bounded by $\hat{R} \leq \delta L_i$ which results in

$$R \leq \rho_f \delta L_i. \tag{55}$$

The bound is propagated through Lemma 11 and Theorem 13 to obtain quality guarantees on the reconstructed surface $\hat{\mathcal{M}}$.

Using $\hat{R} \leq \delta L_i$ with $\delta = 2\epsilon$, we can obtain $R \leq 1.38\delta L_i$ or $|R - \hat{R}| \leq .76\epsilon$ for $\epsilon \leq .0047$ as opposed to the original $\epsilon \leq .002$ as demonstrated in Figure 3.

The bound on R given in [18] may also be used.

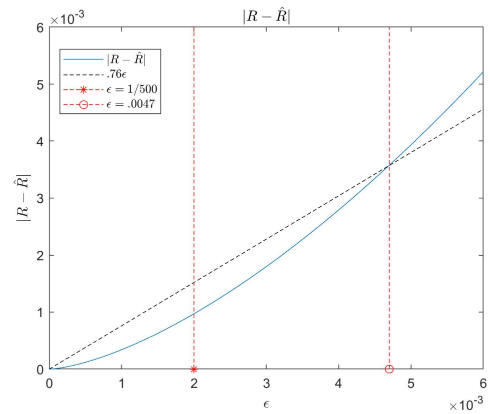

Figure 3: The bound on $|R - \hat{R}|$ as a function of ϵ for $L_i = 1$, $\epsilon = 1/500$ as in [12] along with the larger $\epsilon = .0047$ which gives the same quality guarantee.

5. CONCLUSION

We presented a formula for the difference between the orthoradius and circumradius of a weighted triangle in terms of edge lengths and point weights. As far as we know, this is the only formula in the literature expressed in terms of these quantities. Numerous publications rely on previously published bounds, and we believe this new form will be both simpler to use and give better results. As many meshing methods rely on the Delaunay/Voronoi mesh, it is desirable to understand how a Delaunay mesh changes with respect to vertex insertion and perturbation, and weight perturbation. A formula for the difference between the orthoradius and circumradius in terms of edge lengths and point weights is beneficial as these are fundamental quantities which enables a more immediate determination of how the perturbation of a point location or weight affects this difference. We applied the difference formula to the VoroCrust algorithm to show that the same quality guarantees can be obtained under looser sampling conditions.

This material is based upon work supported by the U.S. Department of Energy, Office of Science, Office of Advanced Scientific Computing Research (ASCR), Applied Mathematics Program.. Sandia National Laboratories is a multi-program laboratory managed and operated by National

Technology and Engineering Solutions of Sandia, LLC., a wholly owned subsidiary of Honeywell International, Inc., for the U.S. Department of Energy's National Nuclear Security Administration under contract DE-NA-0003525. This paper describes objective technical results and analysis. Any subjective views or opinions that might be expressed in the paper do not necessarily represent the views of the U.S. Department of Energy or the United States Government.

References

[1] Cheng S.W., Dey T.K., Shewchuk J. *Delaunay Mesh Generation*. CRC Press, 2012

[2] Devillers O., Teillaud M. "Perturbations for Delaunay and Weighted Delaunay 3D Triangulations." *Computational Geometry*, vol. 44, 160–168

[3] Bernal J. "REGTET: A Program for Computing Regular Tetrahedralizations." *National Institute of Standards and Technology Internal Report*, vol. 6786, 2001

[4] Cignoni P., Montani C., Scopigno R. "DeWall: A Fast Divide and Conquer Delaunay Triangulation Algorithm in Ed." *Computer-Aided Design*, vol. 30, 5: 333–341, 1998

[5] Edelsbrunner H., Shah N. *Incremental Topological Flipping Works for Regular Triangulations*. Proceedings of the eight annual symposium on Computation geometry, Berlin, Germany, June 10-12, 1998

[6] Fang T.P., Piegl L.A. "Delaunay Triangulation in Three Dimensions." *Computer Graphics and Applications, IEEE*, vol. 15, 5:62–69, 1995

[7] Katajainen J., Koppinen K. "Constructing Delaunay Triangulations by Merging Buckets in Quadtree Order." *Fundamenta Informaticae*, vol. XI, 275–288, 1988

[8] Park S., Lee S., Kim J. "The Delaunay Triangulation by Grid Subdivision." *Lecture Notes in Computer Science*, vol. 3482, 385–429, 2005

[9] Yvinec M., Boissonnat J.D. *Algorithmic Geometry*. Cambridge University Press, 1998

[10] Goes F.d., Memari P., Mullen P., Desbrun M. "Weighted Triangulations for Geometry Processing." *ACM Trans. Graph.*, vol. 33, no. 3, 2014. URL `https://doi.org/10.1145/2602143`

[11] Engwirda D. "Generalised Primal-Dual Grids for Unstructured Co-Volume Schemes." *CoRR*, vol. abs/1712.02657, 2017. URL `http://arxiv.org/abs/1712.02657`

[12] Abdelkader A., Bajaj C.L., Ebeida M.S., Mahmoud A.H., Mitchell S.A., Owens J.D., Rushdi A.A. "Sampling Conditions for Conforming Voronoi Meshing by the VoroCrust Algorithm." B. Speckmann, C.D. Tóth, editors, *34th International Symposium on Computational Geometry (SoCG 2018)*, vol. 99 of *Leibniz International Proceedings in Informatics (LIPIcs)*, pp. 1:1–1:16. Schloss Dagstuhl–Leibniz-Zentrum fuer Informatik, Dagstuhl, Germany, 2018

[13] Abdelkader A., Bajaj C.L., Ebeida M.S., Mahmoud A.H., Mitchell S.A., Owens J.D., Rushdi A.A. "VoroCrust: Voronoi Meshing Without Clipping." *ACM Trans. Graph.*, vol. 39, no. 3, May 2020. URL `https://doi.org/10.1145/3337680`

[14] Amenta N., Choi S., Kolluri R.K. "The Power Crust." p. 249–266, 2001

[15] Amenta N., Choi S., Kolluri R.K. "The Power Crust, Unions of Balls, and the Medial Axis Transform." *Computational Geometry*, vol. 19, 127–153, 2001

[16] Chazal F., Lieutier A. "Smooth Manifold Reconstruction from Noisy and Non-uniform Approximation with Guarantees." *Computational Geometry*, vol. 40, no. 2, 156–170, 2008

[17] Hummel M.H. "Delaunay-Laguerre Geometry for Macromolecular Modeling and Implicit Solvation." *Doctoral Dissertation*, 2014

[18] Jean-Daniel Boissonnat S.O. "Provably Good Sampling and Meshing of Surfaces." *Graphical Models, Elsevier*, vol. 67, 405–451, 2005